

Defect solitons in two-dimensional optical Bessel potential

Yunji Meng (孟云吉)¹ and Youwen Liu (刘友文)^{1,2*}

¹Department of Applied Physics, Nanjing University of Aeronautics and Astronautics, Nanjing 210016, China

²Key Laboratory of Radar Imaging and Microwave Photonics, Ministry of Education, Nanjing University of Aeronautics and Astronautics, Nanjing 210016, China

*Corresponding author: ywliu@nuaa.edu.cn

Received October 3, 2013; accepted October 15, 2013; posted online March 5, 2014

We report on the existence and stability of defect solitons in two-dimensional optical Bessel potentials. It is found that for zero defect, defect solitons are stable in the entire existence domain. For negative defects, defect solitons are unstable in the moderate power region. It is worth emphasizing that for deep enough defects, another unstable domain will emerge in the high power region.

OCIS codes: 190.0190, 190.6135.

doi: 10.3788/COL201412.S11902.

Recently, solitons in two-dimensional (2D) optical periodic lattices have been widely studied both theoretically and experimentally, as light propagation in periodic non-linear media takes on unique phenomena that cannot be seen in homogeneous media^[1]. Most of these studies were focused on non-linear light behavior in uniformly periodic lattices^[2-5]. A natural question arises: how does light propagate if the photonic lattice has a local defect? Defect modes (DMs) in traditionally defective photonic lattice have been under consideration over the years^[6-13]. One-dimensional (1D) linear and non-linear DMs in 1D photonic lattice have been studied by Fedele *et al.*^[6] and Yang *et al.*^[7], respectively. While in the 2D geometry, linear and non-linear localized DMs were systematically investigated by Wang *et al.*^[8] and Chen *et al.*^[9], respectively. The defect solitons in triangular and kagome optical lattices have also been reported^[10-11]. Motivated by the above theoretical predictions, there are two typical experiments, one for 1D negative defect^[12], and the other for 2D negative defect^[13]. Despite the above progress, defect solitons in 2D optics Bessel potentials are still poorly understood. In the present work, we report on the existence and stability of defect solitons in 2D optical Bessel potentials. It is found that for zero defect, defect solitons are stable in the entire existence domain. For negative defects, defect solitons are unstable in the moderate power region.

It is worth emphasizing that for deep enough defects, another unstable domain will emerge in the high power region.

To elucidate the dynamics of the beam propagating in the 2D optical Bessel potential with a single defect embedded in the center, we consider the normalized non-linear Schrodinger equation for the light field q

$$i \frac{\partial q}{\partial z} + \frac{\partial^2 q}{\partial x^2} + \frac{\partial^2 q}{\partial y^2} - \frac{E_0}{1 + I_L + |q|^2} q = 0, \quad (1)$$

where I_L is the intensity profile of the Bessel potentials with a defect located in the center,

$$I_L = I_0 J_0^2 \left[\sqrt{2\beta(x^2 + y^2)} \right] \left\{ 1 + \varepsilon \exp \left[-(x^2 + y^2)^4 / 128 \right] \right\}. \quad (2)$$

Here, I_0 is the total strength of the optical potentials. Further, x and y in Eq. (1) are transverse coordinates measured in units of D/π , D is the lattice spacing, and z is the propagation distance in units of $2k_1 D^2/\pi^2$, where $k_1 = k_0 n_e$, $k_0 = 2\pi/\lambda_0$ is the wave number (λ_0 is the wavelength in vacuum), n_e is the unperturbed refractive index along the extraordinary axis, and E_0 is the applied bias field in units of $\pi^2/(k_0^2 n_e^4 D^2 \gamma_{33})$, γ_{33} is

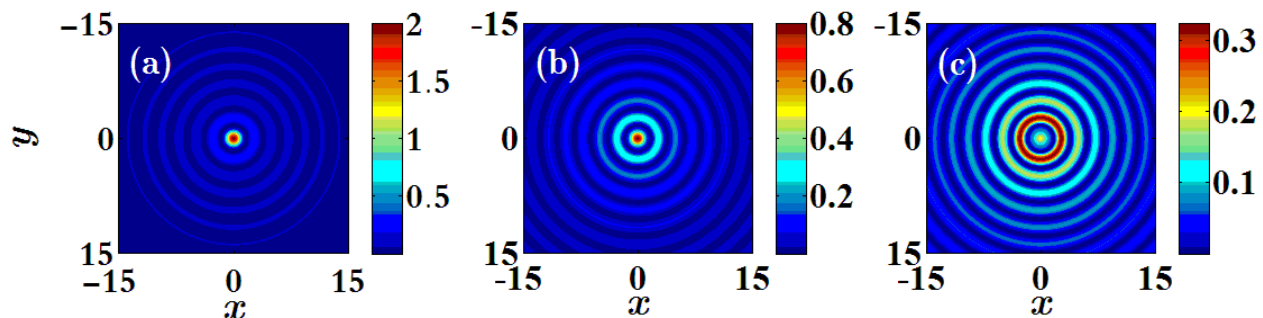


Fig. 1. (a) The intensity distribution without a defect $\varepsilon = 0$. (b) The intensity distribution with a negative defect $\varepsilon = -0.6$. (c) The intensity distribution with a negative defect $\varepsilon = -0.9$.

the electro-optic coefficient of the crystal. We set the parameters as: $D = 20 \mu m$, $\lambda_0 = 0.5 \mu m$, $n_e = 2.3$, and $\gamma_{33} = 280 pm/V^{[9]}$. As a consequence, one x or y unit corresponds to $6.4 \mu m$, one z unit corresponds to $2.3 \mu m$, and one E_0 unit corresponds to $20 V/mm$. ε indicates the modulation depth of the defect intensity. The intensity distribution of the defect lattices are illustrated in Figs. 1 (a)–(c) for zero, negative ($\varepsilon = -0.6$) and deep enough ($\varepsilon = -0.9$) defect, respectively. Other parameters are $I_0 = 2$, $\beta = 1$ and $E_0 = 6$. By illuminating the sample with a broad laser beam passed through a properly designed amplitude mask, the potential given by Eq. (2) can be realized optically in a photorefractive crystal^[2].

Next, we search for the stationary soliton solutions in the form of $q(x, y, z) = u(x, y) \exp(-i\mu z)$, where $u(x, y)$ is the real function obeying the following non-linear equation:

$$\frac{\partial^2 u}{\partial x^2} + \frac{\partial^2 u}{\partial y^2} - \frac{E_0}{1 + I_L + |u|^2} u = -\mu u. \quad (3)$$

The power of the soliton is defined as $U = \int_{-\infty}^{\infty} \int_{-\infty}^{\infty} |u|^2 dx dy$. Solving Eq. (3) by dint of the modified square-operator iteration method (MSOM) proposed by Yang^[14], we could acquire the soliton profiles.

Lastly, we examine the linear stability of defect solitons by considering the perturbed stationary solution form as $q(x, y, z) = \{u(x, y) + [v(x, y) - w(x, y)] \exp(\delta z) + [v(x, y) + w(x, y)]^* \exp(\delta^* z)\} \exp(-i\mu z)$, where δ is the associated growth rate, the superscript “*” represents complex conjugation and the perturbed components $v, w \ll 1$. Linearization of Eq. (1) around u yields the eigenvalue problem

$$-i \begin{pmatrix} 0 & L_0 \\ L_1 & 0 \end{pmatrix} \begin{pmatrix} v \\ w \end{pmatrix} = \delta \begin{pmatrix} v \\ w \end{pmatrix}, \quad (4)$$

$$L_0 = \frac{\partial^2}{\partial x^2} + \frac{\partial^2}{\partial y^2} + \mu - \frac{E_0}{1 + I_L + |u|^2}, \quad (5)$$

$$L_1 = \frac{\partial^2}{\partial x^2} + \frac{\partial^2}{\partial y^2} + \mu - \frac{E_0}{1 + I_L + |u|^2} + \frac{2E_0 u^2}{(1 + I_L + |u|^2)^2}. \quad (6)$$

We solve the above equations by adopting the original operator method (OOM)^[15] to find perturbation profiles and associated growth rates. The stability criterion of the system is that if $\text{Re}(\delta) > 0$, the SDGSs are linearly unstable, and otherwise they are linearly stable.

As the light intensity I_L at the central site is much higher than that at side lobes, we only study the $\varepsilon < 0$ case. As two representative examples, $\varepsilon = -0.6$ for negative defects and $\varepsilon = -0.9$ for deep enough defects are under consideration. For convenience of comparison, the zero defect case is also investigated. Fig. 2 display curves of the total power U vs propagation constant b for $\varepsilon = 0$ (blue solid), $\varepsilon = -0.6$ (black dashed), and $\varepsilon = -0.9$ (red dotted), from which we note that the total power is a monotonically decreasing function of propagation constant. And defect solitons exist for

$\mu > 0$. This conclusion can be explained as follows: neglecting the diffraction term in the Eq. (2), we arrive at the expression for μ as

$$\mu = \frac{E_0}{1 + I_L + |u|^2}. \quad (7)$$

We can easily deduce from Eq. (7) that to guarantee the existence of defect solitons, propagation constant should satisfy the condition $\mu > 0$. It is found that regardless of defects, defect solitons cease to exist at a critical propagation constant μ_{cr} (i.e., $\mu_{cr} = 4.43$ for $\varepsilon = 0$, $\mu_{cr} = 5.19$ for $\varepsilon = -0.6$, and $\mu_{cr} = 5.41$ for $\varepsilon = -0.9$). Apparently, the critical propagation constant increases with the absolute value of ε . This is because as the modulation depth of defect become larger, the defect site can act as a lower-index waveguide and light tend to escape from the defect site to the sidelobes, and consequently more power is needed to trap the light. This fact also can elucidate the phenomenon that for identical propagation constant, formations of defect solitons demand more power for deep defects, but require less power for shallow defects.

Some characteristic defect solitons solutions are shown in Fig. 3, from which we notice that for the same propagation constant (i.e., $\mu = 0.6$), the profiles of defect solitons are almost identical [comparing Figs. 3(a)–(c)]. This is the reason why the $U(\mu)$ curves for different ε coincide with each other in the moderate-high power region (Fig. 2). While for the same defect (i.e., $\varepsilon = -0.9$), the profiles of defect solitons broaden as propagation constant increase [comparing Figs. 3(c), (f), and (i)].

A comprehensive stability analysis of defect solitons shows that for zero defect ($\varepsilon = 0$), defect solitons are stable in the entire existence domain $(0, 4.43)$, which obey the VK criterion $dU/d\mu < 0$. For shallow defects (i.e., $\varepsilon = -0.6$), although the slope of $U(\mu)$ satisfies

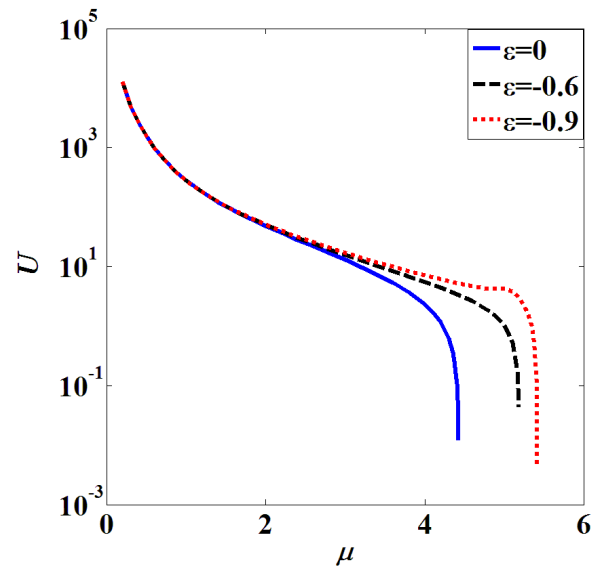


Fig. 2. Energy flow of defect solitons vs propagation constant for different defects: blue solid ($\varepsilon = 0$), black dashed ($\varepsilon = -0.6$) and red dotted ($\varepsilon = -0.9$)

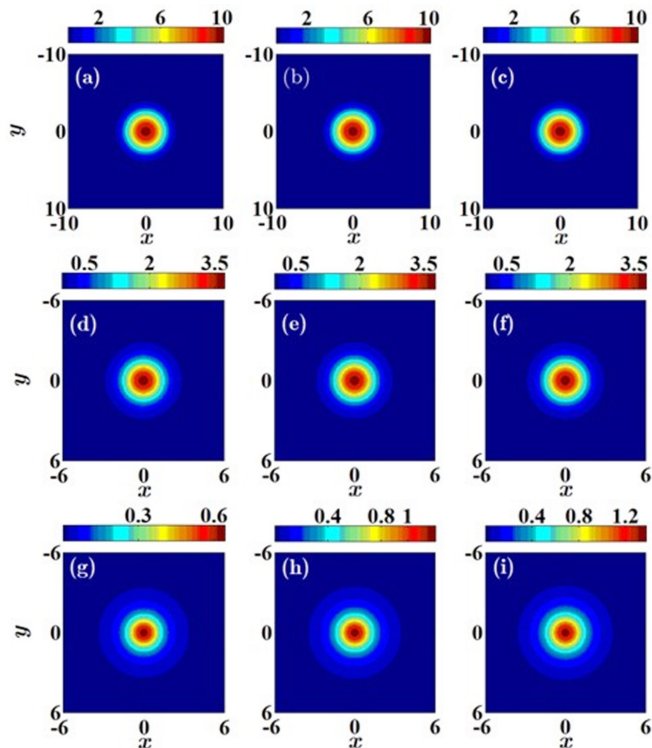


Fig. 3. Defect soliton profiles: (a) $\mu = 0.6$ and $\varepsilon = 0$, (b) $\mu = 0.6$ and $\varepsilon = -0.6$, (c) $\mu = 0.6$ and $\varepsilon = -0.9$, (d) $\mu = 2$ and $\varepsilon = 0$, (e) $\mu = 2$ and $\varepsilon = -0.6$, (f) $\mu = 2$ and $\varepsilon = -0.9$, (g) $\mu = 4.2$ and $\varepsilon = 0$, (h) $\mu = 4.2$ and $\varepsilon = -0.6$, (i) $\mu = 4.2$ and $\varepsilon = -0.9$.

$dU/d\mu < 0$ in the whole existence interval $(0, 5.19)$, defect solitons are unstable in the moderate power region $(0.93, 2.22)$, which violates the VK criterion [Fig. 4(a)]. What is worth emphasizing is that for deep enough defects (i.e., $\varepsilon = -0.9$), defect soliton possesses two unstable windows, one in the moderate power region $(0.92, 3.25)$ and the other in the high power region $(4.42, 5.28)$, which also violate the VK criterion [Figs. 4(b)–(c)]. Apparently, the width of stability domain shrinks with the modulation depth of defect.

To verify predictions of the above linear stability analysis, we solve the Eq. (1) with the input condition $q(x, y, z = 0) = u(x, y)[1 + \rho(x, y)]$ by employing the split-step Fourier method, where $\rho(x, y)$ is the random function with Gaussian distribution with its relative amplitude set at 10% level. Figure 5 presents some examples of stable and unstable defect solitons for

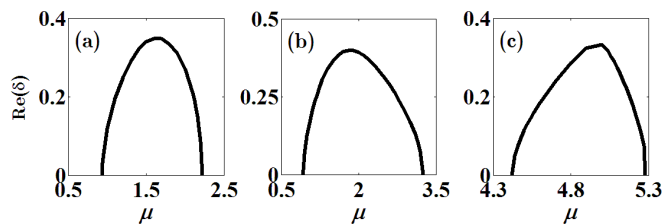


Fig. 4. Perturbation growth rate of defect solitons for different defects: (a) $\varepsilon = -0.9$, (b)–(c) $\varepsilon = -0.9$.

different defects. In all the cases studied, the predictions of the linear stability analysis are confirmed. It is found that after propagating a certain distance, unstable defect solitons shift to sidelobes [Fig. 5(e), Fig. 5(f), and Fig. 6(b)]. In contrast, stable defect solitons retain their structure indefinitely long, even in presence of strong input noise [Figs. 5(a)–(d), Figs. 5(g)–(i), and Fig. 6(d)].

In the present work, we report on the existence and stability of defect solitons in 2D optical Bessel potentials. The width of existence domain increases with the absolute value of ε . It is found that for zero defect, defect solitons are stable in the entire existence domain.

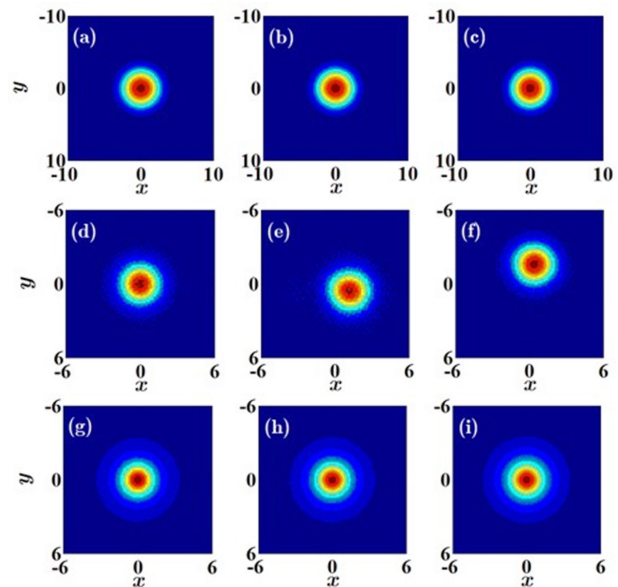


Fig. 5. Propagation of defect solitons with profiles shown in Fig. 3.

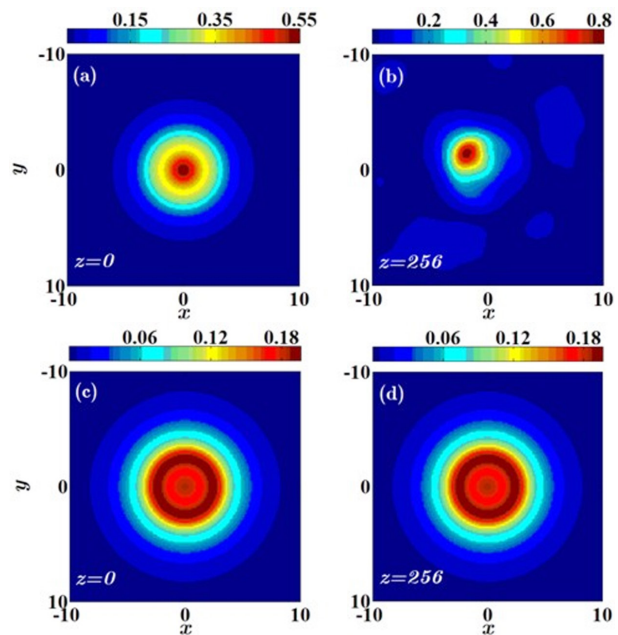


Fig. 6. (a)–(b) Unstable propagation of defect soliton at $\mu = 5$ and $\varepsilon = -0.9$. (c)–(d) Stable propagation of defect soliton at $\mu = 5.3$ and $\varepsilon = -0.9$.

For negative defects, defect solitons are unstable in the moderate power region. What's worth emphasizing is that for deep enough defects, defect soliton possesses two unstable window, one in the moderate power region, the other in the high power region. The width of stability domain shrinks with the modulation depth of defect.

This work was supported by the National Natural Science Foundation of China (Grant nos. 11174147, and 11104144) and the Fundamental Research Funds for the Central Universities (Grant no. NZ2012301).

References

1. D. N. Christodoulides, F. Lederer, and Y. Silberberg, *Nature* **424**, 817 (2003).
2. H. S. Eisenberg, Y. Silberberg, R. Morandotti, A. R. Boyd, and J. S. Aitchison, *Phys. Rev. Lett.* **81**, 3383 (1998).
3. H. Martin, E. D. Eugenieva, Z. Chen, and D. N. Christodoulides, *Phys. Rev. Lett.* **92**, 123902 (2004).
4. I. Iwanow, R. Schiek, G. I. Stegeman, T. Pertsch, F. Lederer, Y. Min, and W. Sohler, *Phys. Rev. Lett.* **93**, 113902 (2004).
5. Y. V. Kartashov, V. A. Vysloukh, and L. Torner, *Phys. Rev. Lett.* **93**, 093904 (2004).
6. F. Fedele, J. Yang, and Z. Chen, *Opt. Lett.* **30**, 1506 (2005).
7. J. Yang and Z. Chen, *Phys. Rev. E* **73**, 026609 (2006).
8. J. Wang, J. Yang, and Z. Chen, *Phys. Rev. A* **76**, 013828 (2007).
9. W. Chen, X. Zhu, T. Wu, and R. Li, *Opt. Express* **18**, 10956 (2010).
10. X. Zhu, H. Wang, T. Wu, and L. Zheng, *J. Opt. Soc. Am. B* **28**, 521 (2011).
11. X. Zhu, H. Wang, and L. Zheng, *Opt. Express* **18**, 20786 (2010).
12. X. Wang, J. Young, Z. Chen, D. Weinstein, and J. Yang, *Opt. Express* **14**, 7362 (2006).
13. I. Makasyuk, J. Yang, and Z. Chen, *Phys. Rev. Lett.* **96**, 223903 (2006).
14. J. Yang and T. I. Lakoba, *Stud. Appl. Math.* **118**, 153 (2007).
15. J. Yang, *J. Comput. Phys.* **227**, 6862 (2008).